



Published in final edited form as:

Science. 2017 November 10; 358(6364): 761–764. doi:10.1126/science.aao5894.

Lewis Acid Enhancement by Hydrogen-Bond Donors for Asymmetric Catalysis**

Steven M. Banik[‡], Anna Levina[‡], Alan M. Hyde, and Eric N. Jacobsen*

Department of Chemistry and Chemical Biology, Harvard University, Cambridge MA 02138, USA

Abstract

Small molecule dual hydrogen-bond (H-bond) donors such as ureas, thioureas, squaramides, and guanidinium ions enjoy widespread use as effective catalysts for promoting a variety of enantioselective reactions. However, these catalysts are only weakly acidic, and therefore require highly reactive electrophilic substrates in order to be effective. We introduce here a mode of catalytic activity with chiral H-bond donors that enables enantioselective reactions of relatively unreactive electrophiles. Squaramides are shown to interact with silyl triflates by binding the triflate counterion to form a stable yet highly Lewis acidic complex. The silyl triflate-chiral squaramide combination promotes the generation of oxocarbenium intermediates from acetal substrates at low temperatures. Enantioselectivity in nucleophile additions to the cationic intermediates is then controlled through a network of non-covalent interactions between the squaramide catalyst and the oxocarbenium triflate.

Main Text

Chiral hydrogen-bond (H-bond) donors can catalyze enantioselective nucleophile-electrophile addition reactions either by direct complexation with neutral electrophiles, or by anion binding to generate chiral ion pair intermediates (Fig. 1A)(1,2). However, because of the generally weak Brønsted acidity of the catalysts (3,4), these approaches commonly require highly electrophilic substrates with labile carbon-heteroatom (σ or π) bonds (2). We considered whether the anion-binding principle could be applied in a fundamentally different way, to enhance the reactivity of Lewis acids such as silyl triflates through association of a chiral H-bond donor with the triflate. This strategy could enable the generation of highly reactive cationic intermediates from relatively stable precursors, while

**“This manuscript has been accepted for publication in *Science*. This version has not undergone final editing. Please refer to the complete version of record at <http://www.sciencemag.org/>. The manuscript may not be reproduced or used in any manner that does not fall within the fair use provisions of the Copyright Act without the prior, written permission of AAAS.”

*Correspondence to: jacobsen@chemistry.harvard.edu.

[‡]These authors contributed equally to this work.

SUPPLEMENTARY MATERIAL

www.sciencemag.org/content/

Materials and Methods

Tables S1 to S9

Figures S1 to S23

References (35–52)

GC and HPLC Traces

NMR Spectra

still enabling enantiocontrol through non-covalent interactions with the chiral catalyst. We report here the realization of this idea in the discovery of cooperative reactivity between silyl triflates and chiral squaramides, and its application to a series of enantioselective reactions involving oxocarbenium ion intermediates.

Silyl triflates are readily available Lewis acids with broad application in organic synthesis (5,6). The reactivity of these reagents is enhanced through incorporation of more weakly coordinating anionic ligands such as disulfonimides, as demonstrated initially by Ghosez in racemic Diels-Alder reactions (7,8,9). List and coworkers extended this advance to enantioselective catalysis through the design of chiral disulfonimide counteranion that associate with the active silylium species (10, 11). We envisaged an alternative approach wherein association of a chiral H-bond donor with the triflate anion would generate a charge-separated complex with enhanced Lewis acidity relative to silyl triflate alone. Given the outstanding chiral induction properties of H-bond donors in reactions of ion-pair intermediates, this approach would open the door to a wide variety of enantioselective catalytic reactions. We sought to apply this activation principle to the generation of oxocarbenium ions from stable acetals for the Mukaiyama aldol reaction, a prototypical Lewis-acid promoted process (12,13); the trimethylsilyl enol ether derived from acetophenone and 4-bromobenzaldehyde dibenzyl acetal (**1a**) were selected as model substrates (Fig. 1B). Under the optimized reaction conditions ($-78\text{ }^{\circ}\text{C}$, methyl *tert*-butyl ether; MTBE), the combination of chiral squaramide (14) derivatives (**5**) and silyl triflates (e.g. TBSOTf, 50 mol%) was uniquely effective at promoting the enantioselective reaction; no reaction was observed with TBSOTf either alone or in the presence of representative urea (**3**) and thiourea (**4**) catalysts under the same conditions. Reactivity and enantioselectivity were strongly responsive to the expanse of the arylpyrrolidine substituent on the squaramide, with pyrenyl catalyst **5e** being optimal (100% conversion, 88% e.e.). The importance of the H-bond donor motif of the catalyst was established through evaluation of **6e**, the *N,N'*-dimethyl squaramide analog of **5e**, which promoted the aldol addition but afforded nearly racemic product. This observation of moderate reactivity but negligible enantioselectivity with **6e** suggests that the Lewis basic properties of the squaramide catalysts may play a role in enhancing the Lewis acidity of the silyl triflate (15,16), but that the H-bond donor properties are essential for effective stereochemical control.

This strategy for generating oxocarbenium ion intermediates from stable acetals and engaging them in enantioselective alkylation reactions was readily extended to other classes of nucleophiles (Fig. 1C). With **5e** and TBSOTf (17) as the silyl triflate promoter, allyl silane, silyl enol ether, and silyl ketene acetal nucleophiles engaged in highly enantioselective reactions with electrophiles derived from **1** (for expanded substrate scope, see fig. S1). Effective enantiocontrol in alkylations of oxocarbenium ions was thus achieved with alkylating reagents spanning five orders of magnitude of nucleophilicity ($N=3.78$ to $N=9.00$). (18)

We sought to test the generality of H-bond donor-silyl triflate cooperativity in a highly demanding synthetic context, and selected (4+3) cycloadditions for examination. These reactions provide an attractive approach to functionalized 7-membered carbocyclic frameworks (19,20), and limited success in the development of enantioselective, catalytic

variants has been achieved despite important pioneering efforts (21,22,23). A protocol analogous to the one described above for Mukaiyama aldol-type reactions of acetals (24,25) was applied successfully to the reaction of oxyallyl cation precursors (**7**) with furan derivatives (**8**) to generate bicyclic (4+3) cycloadducts (**9**) in good yield and high enantioselectivity as single diastereomers (Fig. 2). Substituted oxyallyl cation precursors and 3-substituted furans in particular afforded products with the highest enantioselectivity (**9b-k**). As observed in the Mukaiyama-type reactions, squaramides were uniquely effective as catalysts and a strong dependence of reactivity and enantioselectivity on catalyst structure was observed, with squaramide derivative **5e** again affording optimal results (Fig. S7).

The results presented in Figures 1 and 2 reveal that the cooperative action of squaramide H-bond donors with silyl triflates can serve to catalyze a variety of enantioselective transformations of acetals, and may offer a general approach to catalytic generation and asymmetric reaction of cationic intermediates from relatively stable precursors. Given the potential utility of this approach, we undertook a careful analysis of the (4+3) cycloaddition to glean insight into the underlying catalytic mechanism. The reaction that generates bicyclic adduct **9g** was selected for kinetic analysis, as it proceeds with rates conveniently monitored by in situ IR spectroscopy. A first-order kinetic dependence on acetal and a zero-order dependence on furan were observed (Figs. S14 and S15), together with saturation kinetics with respect to [TESOTf] (Fig. 3A, left) and a first-order dependence on squaramide **5e**. The recently reported method of Burés for determination of reaction order in [**5e**] proved particularly convenient in this regard (Fig. 3A, right) (26).

The kinetic data for the (4+3) cycloaddition are consistent with a pre-equilibrium formation of a resting-state complex between the squaramide catalyst and TESOTf, and rate-limiting reaction of this complex with the acetal substrate (27). In order to assess this model and the nature of this complex, the interaction between the H-bond donor catalyst and TESOTf was examined spectroscopically. Titration experiments were performed with catalyst **5g**, which provided well-resolved ¹H NMR spectra and displayed similar kinetic behavior to **5e** (28). Application of the method of continuous variation revealed a 1:1 binding interaction between TESOTf and **5g** (Fig. 3B). In this manner, 1:1 binding was established between different squaramide and triflate sources, and the binding constants were determined from titration experiments quantified by ¹H NMR (Fig. 3C). As expected given the known anion-binding properties of squaramides (29) NBu₄OTf forms a stable complex with **5g** in CD₂Cl₂ (Fig. 4c, entry 1). However, TESOTf was found to bind 4000 times more tightly than NBu₄OTf (Fig. 4c, entry 2), an indication that simultaneous binding of both the triflate and the trialkyl silyl component may be occurring in the complex. Further evidence for a direct squaramide-silicon interaction is provided by the observation that the dimethylated squaramide derivative **6g**, which lacks H-bond donor capabilities, also forms a complex with TESOTf. Titration of a solution of **5g** in MTBE at -78 °C with TESOTf was also monitored by in situ IR, with disappearance of the absorbances attributed to the squaramide carbonyl groups observed upon addition of TESOTf (Fig. 3D) (30). Taken together, the kinetic and binding studies are consistent with an unexpectedly strong 1:1 complex between TESOTf and **5** as the resting state of the catalyst in the reactions outlined in Figures 2 and 3.

Computational modeling of the 1:1 complex between **5g** and TMSOTf using density functional theory (DFT) revealed a minimum energy structure in which the silyl triflate is dissociated heterolytically, with the triflate anion engaged by nearly symmetrical dual H-bonding interactions (1.67 Å and 1.68 Å), and the corresponding silylium cation associated covalently with the more Lewis basic of the carbonyls in the squaramide moiety (Fig. 3E). This dual interaction mode may account for the enhanced affinity of the squaramide for the silyl triflate relative to tetraalkylammonium triflate. Under the conditions of catalysis, the activated silylium species may be associated directly with the squaramide such as in Figure 3E and/or with the solvent. In either case, the complex between **5** and R₃SiOTf is expected to be more Lewis acidic than R₃SiOTf alone due to the stabilization of the triflate anion by the H-bond donor.

The catalytic cycle depicted in Figure 4A is consistent with the kinetic and binding studies outlined above. The silyl triflate-squaramide complex serves as the resting state of the catalyst and as a potent Lewis acid that promotes acetal ionization. Post-rate-determining reaction of the oxyallyl cation intermediate with the furan affords the (4+3) cycloadduct. Based on the observation that similar e.e.'s are obtained with different trialkyl silyl triflate promoters (Fig. S5), it is proposed that the enantioselectivity-determining step occurs after formation of the oxyallyl cation and involves the reaction with furan. The basis for stereoinduction in the cycloaddition reaction was probed computationally using DFT with **5f** as the squaramide catalyst. Consistent with prior studies on (4+3) cycloadditions of furan and alkoxy silyloxyallyl cations (31,32), the calculations converge on a stepwise mechanism involving initial nucleophilic attack by furan at the vinyl terminus of the oxyallyl cation followed by ring closure (Fig. S22). The structures corresponding to the lowest-energy transition states for the first, enantioselectivity-determining C–C bond-forming step en route to the major and minor enantiomers of product are presented in Figs. 4B and 4C, respectively. Single point calculations at the M062X/6-31+G(d,p) level of theory reproduce both the sense and magnitude ($E_{\text{calc}}^{\ddagger} = 1.28$ kcal/mol) of enantioinduction determined experimentally. Both transition states display a network of hydrogen-bonding interactions between the oxyallyl fragment and the triflate counterion, as well as between furan and the amide backbone of the catalyst. However, the positioning of the furan nucleophile in proximity to the aromatic substituent of the catalyst in **I** (major) suggests a stabilizing interaction between the furan and the catalyst. Such an interaction is absent in **II** (minor), and may thus be a key factor responsible for enantioselectivity (33,34).

The interaction between simple silyl triflates and squaramide H-bond donors produces a highly reactive Lewis acid complex capable of activating acetals to produce chiral catalyst-associated oxocarbenium ion intermediates. Enantioselectivity in reactions of these intermediates can be achieved through the interplay of non-covalent interactions between the H-bond donor catalyst and both components of the ion pair. Enhancement of the intrinsic reactivity of Lewis acids represents a potentially powerful strategy for the development of asymmetric reactions proceeding through high-energy cationic intermediates.

Supplementary Material

Refer to Web version on PubMed Central for supplementary material.

Acknowledgments

We gratefully acknowledge financial support from the NIH (grant GM043214 to E.N.J. and a postdoctoral fellowship to A.M.H.) and the NSF (predoctoral fellowship to S.M.B.), and helpful discussions with Prof. Michael Harmata (University of Missouri). Crystallographic data for compounds **9b** and **S9e** are available free of charge from the Cambridge Crystallographic Data Centre under reference CCDC 1578582 and CCDC 1578581, respectively. Additional optimization and mechanistic data are provided in the supplementary materials.

References and Notes

1. Doyle A, Jacobsen EN. Small molecule H-bond donors in asymmetric catalysis. *Chem Rev.* 2007; 107:5713–5743. [PubMed: 18072808]
2. Brak K, Jacobsen EN. Asymmetric ion-pairing catalysis. *Angew Chem Int Ed.* 2013; 52:534–561.
3. Jakab G, Tancon C, Zhang Z, Lippert KM, Schreiner PR. (Thio)urea organocatalyst equilibrium acidities in DMSO. *Org Lett.* 2012; 14:1724–1727. [PubMed: 22435999]
4. Ni X, Li X, Wang Z, Cheng J-P. Squaramide equilibrium acidities in DMSO. *Org Lett.* 2014; 16:1786–1789. [PubMed: 24606030]
5. Dilman AD, Ioffe SL. Carbon–carbon bond forming reactions mediated by silicon Lewis acids. *Chem Rev.* 2003; 103:733–772. [PubMed: 12630851]
6. Hosomi, A., Miura, K. *Acid Catalysis in Modern Organic Synthesis.* Yamamoto, H., Ishihara, K., editors. Wiley-VCH; Weinheim, Germany: 2008. p. 469-516.
7. Mathieu B, Ghosez L. Trimethylsilyl bis(trifluoromethanesulfonyl)imide as a tolerant and environmentally benign Lewis acid catalyst of the Diels–Alder reaction. *Tetrahedron.* 2002; 58:8219–8226.
8. Hara K, Akiyama R, Sawamura M. Strong counteranion effects on the catalytic activity of cationic silicon Lewis acids in Mukaiyama aldol and Diels–Alder reactions. *Org Lett.* 2005; 7:5621–5623. [PubMed: 16321006]
9. Klare HFT, Bergander K, Oestreich M. Taming the silylium ion for low-temperature Diels–Alder reactions. *Angew Chem Int Ed.* 2009; 48:9077–9079.
10. James T, van Gemmeren M, List B. Development and applications of disulfonimides in enantioselective organocatalysis. *Chem Rev.* 2015; 115:9388–9409. [PubMed: 26147232]
11. Gatzemeier T, van Gemmeren M, Xie Y, Höfler D, Leutzsch MB, List, Asymmetric Lewis acid organocatalysis of the Diels–Alder reaction by a silylated C–H acid. *Science.* 2016; 351:949–952. [PubMed: 26917765]
12. Matsuo, J-i, Murakami, M. The Mukaiyama aldol reaction: 40 years of continuous development. *Angew Chem Int Ed.* 2013; 52:9109–9118.
13. Murata S, Suzuki M, Noyori R. A stereoselective aldol-type condensation of enol silyl ethers and acetals catalyzed by trimethyl trifluoromethanesulfonate. *J Am Chem Soc.* 1980; 102:3248–3249.
14. Malerich JM, Hagihara K, Rawal VH. Chiral squaramide derivatives are excellent hydrogen bond donor catalysts. *J Am Chem Soc.* 2008; 130:14416–14417. [PubMed: 18847268]
15. Storer RI, Aciro C, Jones LH. Squaramides: physical properties, synthesis and applications. *Chem Soc Rev.* 2011; 40:2330–2346. [PubMed: 21399835]
16. Denmark SE, Wynn T. Lewis base activation of Lewis acids: catalytic enantioselective allylation and propargylation of aldehydes. *J Am Chem Soc.* 2001; 123:6199–6200. [PubMed: 11414863]
17. TBSOTf was employed due to ease of handling relative to TMSOTf.
18. Mayr H, Bug T, Gotta MF, Hering N, Irrgang B, Janker B, Kempf B, Loos R, Ofial AR, Remennikov G, Schimmel H. Reference Scales for the Characterization of Cationic Electrophiles and Neutral Nucleophiles. *J Am Chem Soc.* 2001; 123:9500–9512. [PubMed: 11572670]
19. Hoffman HMR. The cycloaddition of allyl cations to 1,3-dienes: general method for the synthesis of seven-membered carbocycles. *New synthetic methods (40).* *Angew Chem Int Ed.* 1984; 23:1–19.
20. Harmata M. The (4+3)-cycloaddition reaction: simple allylic cations as dienophiles. *Chem Commun.* 2010; 46:8886–8903.

21. Harmata M, Ghosh SK, Hong X, Wacharasindhu S, Kirchhoefer P. Asymmetric organocatalysis of 4+3 cycloaddition reactions. *J Am Chem Soc.* 2003; 125:2058–2059. [PubMed: 12590528]
22. Huang J, Hsung RP. Chiral Lewis acid-catalyzed highly enantioselective [4+3] cycloaddition reactions of nitrogen-stabilized oxyallyl cations derived from allenamides. *J Am Chem Soc.* 2005; 127:50–51. [PubMed: 15631443]
23. Villar L, Uria U, Martínez JI, Prieto L, Reyes E, Carrillo L, Vicario JL. Enantioselective Oxidative (4+3) Cycloadditions between Allenamides and Furans through Bifunctional Hydrogen-Bonding/Ion-Pairing Interactions. *Angew Chem Int Ed.* 2017
24. Murray DH, Albizati KF. Ambiphilic reactivity of 1,1-dimethoxyacetone. *Tetrahedron Lett.* 1990; 31:4109–4112.
25. Slightly higher (1–2%) enantioselectivity was obtained using TESOTf instead of TBSOTf in select reactions.
26. Bures J. A simple graphical method to determine the order in catalyst. *Angew Chem Int Ed.* 2016; 55:2028–2031.
27. On the basis of the binding data depicted in Figs. 3C and 3D, rate saturation in the catalytic reaction would be expected to occur at lower [TESOTf] than what is observed in Fig. 3A. One possible explanation for this discrepancy is that the acetal substrate might undergo initial conversion to a mixed sulfonate acetal (i.e., RCH(OMe)(OTf)), which then undergoes ionization to generate the oxocarbenium intermediate (see fig. S16). This scenario fits within the general catalytic cycle proposed in Fig. 4A and does not require any changes to the mechanistic conclusions outlined herein.
28. The enantioselective reaction proceeds most effectively and remains homogeneous in ethereal solvents such as MTBE. However, gel formation was observed at high concentrations. Accordingly, the quantitative binding measurements were carried out in CD₂Cl₂ to ensure complete solubility of all components and to avoid competing reactions between TESOTf and solvent.
29. Amendola V, Bergamaschi G, Boiocchi M, Fabbrizzi L, Milani M. The squaramide versus urea contest for anion recognition. *Chem Eur J.* 2010; 16:4368–4380. [PubMed: 20222093]
30. López KA, Piña MN, Quiñonero D, Ballester P, Morey J. Highly efficient coordination of Hg²⁺ and Pb²⁺ metals in water with squaramide-coated Fe₃O₄ nanoparticles. *J Mater Chem A.* 2014; 2:8796–8803.
31. Krenke EH, Houk KN, Harmata M. Origin of stereoselectivity in the (4 + 3) cycloadditions of chiral alkoxy siloxyallyl cations with furan. *Org Lett.* 2010; (12):444–447. [PubMed: 20063884]
32. Sáez JA, Arnó M, Domingo LR. Lewis acid-catalyzed [4+3] cycloaddition of 2-(trimethyl silyloxy)acrolein with furan. Insight on the nature of the mechanism from a DFT analysis. *Org Lett.* 2003; 5:4117–4120. [PubMed: 14572263]
33. Kennedy CR, Lin S, Jacobsen EN. The cation– π interaction in small-molecule catalysis. *Angew Chem Int Ed.* 2016; 55:12596–12624.
34. Neel AJ, Hilton MJ, Sigman MS, Toste FD. Exploiting non-covalent π interactions for catalyst design. *Nature.* 2017; 543:637–646. [PubMed: 28358089]
35. Zhang H, Lin S, Jacobsen EN. Enantioselective Selenocyclization via Dynamic Kinetic Resolution of Seleniranium Ions by Hydrogen-Bond Donors. *J Am Chem Soc.* 2014; 136:16485–16488. [PubMed: 25380129]
36. Yang W, Du DM. Highly enantioselective Michael addition of nitroalkanes to chalcones using chiral squaramides as hydrogen bonding organocatalysts. *Org Lett.* 2010; 12:5450–5453. [PubMed: 21053936]
37. Gregg BT, Golden KC, Quinn JF. Indium(III)trifluoromethanesulfonates as a mild, efficient catalyst for the formation of acetals and ketals in the presence of acid sensitive functional groups. *Tetrahedron.* 2008; 64:3287–3295.
38. Ayla-Mata F, Barrera-Mendoza C, Jumenez-Vazquez HA, Vargas-Diaz E, Zepeda LG. Efficient preparation of α -ketoacetals. *Molecules.* 2012; 17:13864–13878. [PubMed: 23174902]
39. Takehira S, Masui Y, Onaka M. The Mukaiyama aldol reactions for congested ketones catalyzed by solid acid of tin(IV) ion-exchanged montmorillonite. *Chem Lett.* 2014; 43:498–500.

40. Kamigata N, Udodaira K, Shimizu T. Reactions of sulfonyl chlorides with silyl enol ethers catalyzed by a ruthenium(II) phosphine complex: convenient synthesis of β -keto sulfones. *J Chem Soc, Perkin Trans 1*. 1997; 5:783–786.
41. Berkessel A, Das S, Pekel D, Neudörf JM. Anion-binding catalysis by electron-deficient pyridinium cations. *Angew Chem Int Ed*. 2014; 53:11660–11664.
42. Henry N, Enguehard-Gueffier C, Thery I, Gueffier A. One-pot dual substitutions of bromobenzyl chloride 2-chloromethyl-6-halogenoimidazo[1,2-*a*]pyridine and -[1,2-*b*]pyridazine by Suzuki-Miyaura cross-coupling reactions. *Eur J Org Chem*. 2008; 28:4824–4827.
43. Tofi M, Georgiou T, Montagnon T, Vassilikogiannakis G. Regioselective ortho lithiation of 3-aryl and 3-styryl furans. *Org Lett*. 2005; 7:3347–3350. [PubMed: 16018657]
44. Rivera JM, Martin T, Rebek J Jr. Chiral softballs: Synthesis and molecular recognition properties. *J Am Chem Soc*. 2001; 128:5213–5220.
45. Blackmond DG. Reaction progress kinetic analysis: a powerful methodology for mechanistic studies of complex organic reactions. *Angew Chem Int Ed*. 2005; 44:4302–4310.
46. Zuend SJ, Jacobsen EN. Cooperative catalysis by tertiary amino-thioureas: Mechanism and basis for enantioselectivity of ketone cyanosilylation. *J Am Chem Soc*. 2007; 129:15872–15883. [PubMed: 18052247]
47. Fielding L. Determination of association constants (K_a) from solution NMR data. *Tetrahedron*. 2000; 56:6151–6170.
48. Frisch, MJ., Trucks, GW., Schlegel, HB., Scuseria, GE., Robb, MA., Cheeseman, JR., Scalmani, G., Barone, V., Mennucci, B., Petersson, GA., Nakatsuji, H., Caricato, M., Li, X., Hratchian, HP., Izmaylov, AF., Bloino, J., Zheng, G., Sonnenberg, JL., Hada, M., Ehara, M., Toyota, K., Fukuda, R., Hasegawa, J., Ishida, M., Nakajima, T., Honda, Y., Kitao, O., Nakai, H., Vreven, T., Montgomery, JA., Jr, Peralta, JE., Ogliaro, F., Bearpark, M., Heyd, JJ., Brothers, E., Kudin, KN., Staroverov, VN., Kobayashi, R., Normand, J., Raghavachari, K., Rendell, A., Burant, JC., Iyengar, SS., Tomasi, J., Cossi, M., Rega, N., Millam, JM., Klene, M., Knox, JE., Cross, JB., Bakken, V., Adamo, C., Jaramillo, J., Gomperts, R., Stratmann, RE., Yazyev, O., Austin, AJ., Cammi, R., Pomelli, C., Ochterski, JW., Martin, RL., Morokuma, K., Zakrzewski, VG., Voth, GA., Salvador, P., Dannenberg, JJ., Dapprich, S., Daniels, AD., Farkas, O., Foresman, JB., Ortiz, JV., Cioslowski, J., Fox, DJ. Gaussian 09, Revision A.02. Gaussian, Inc; Wallingford CT: 2009.
49. CYLview, 1.0b. Legault, C. Y: Université de Sherbrooke; 2009. (<http://www.cylview.org>)
50. A.X.S, APEX3. Bruker AXS; Madison, Wisconsin: 2014.
51. Sheldrick GM. Crystal structure refinement with *SHELXL*. *Acta Cryst*. 2008; 64:112–122.
52. Dolomanov OV, Bourhis LJ, Gildea RJ, Howard JAK, Puschmann H. OLEX2: A complete structure solution, refinement and analysis program. *J Appl Cryst*. 2009; 42:339–341.

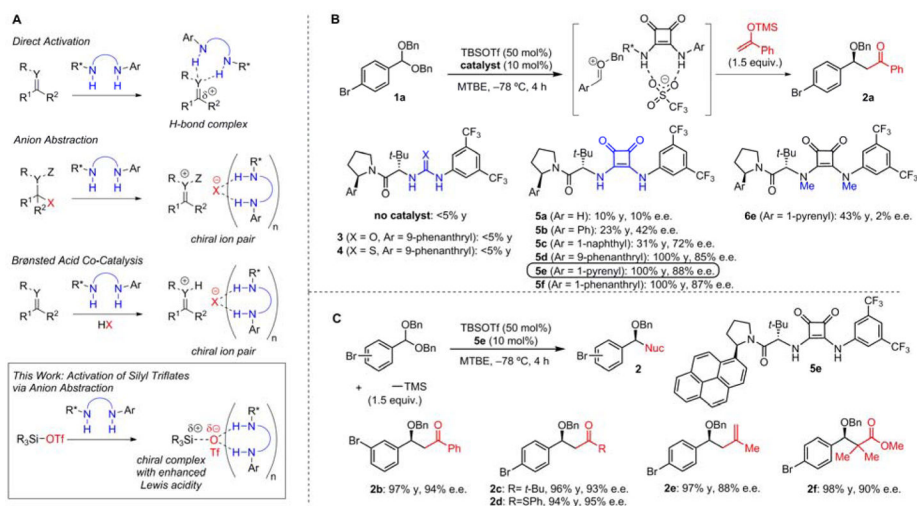


Figure 1. Reactivity concept and reaction development

(A) Existing strategies for electrophile activation using chiral dual hydrogen-bond donor catalysts, and the approach explored in this study using anion binding to generate a reactive, cationic metal or metalloid center as a chiral ion pair. (B) Proof-of-concept in the silyl triflate-promoted Mukaiyama aldol reaction of an acetal, with examples from optimization studies of the chiral squaramide catalysts. (C) Representative examples of enantioselective alkylation reactions of acetals promoted by TBSOTf and catalyzed by **5e**.

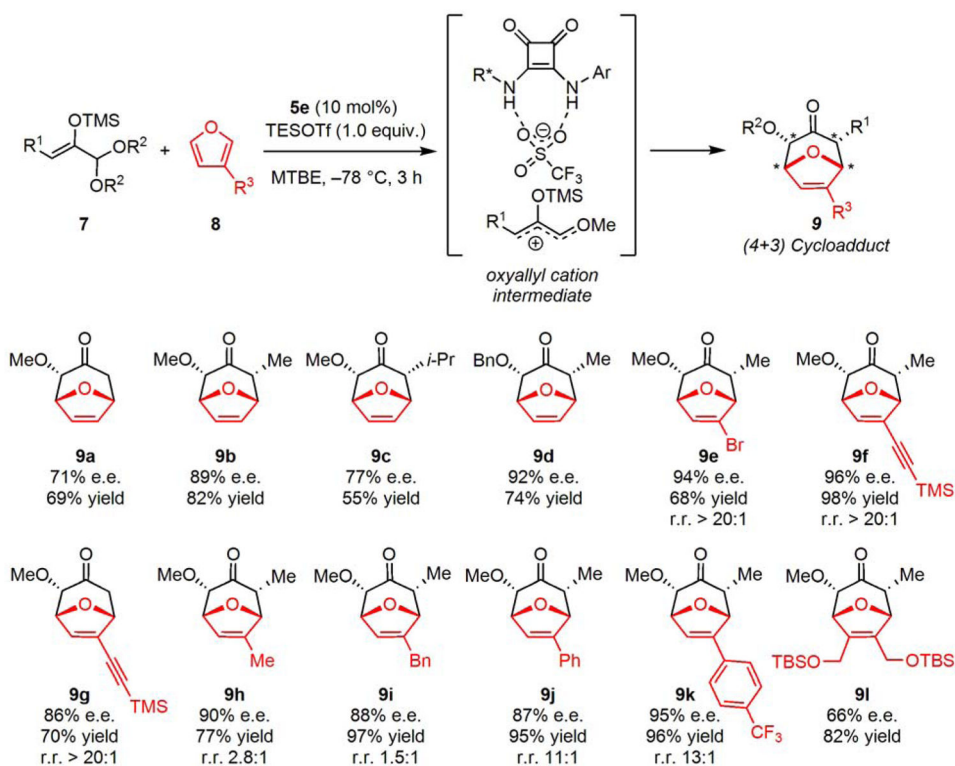


Figure 2. (4+3) Cycloaddition Substrate scope

Cooperative reactivity of squaramide catalysts and silyl triflate Lewis acids in enantioselective (4+3) cycloadditions via oxyallyl cation intermediates, r.r. is the regioisomeric ratio. In all cases, only the indicated diastereomer was detectable. Absolute stereochemistry was assigned by X-ray crystallographic analysis of a crystalline derivative of **9b** and **9e**.

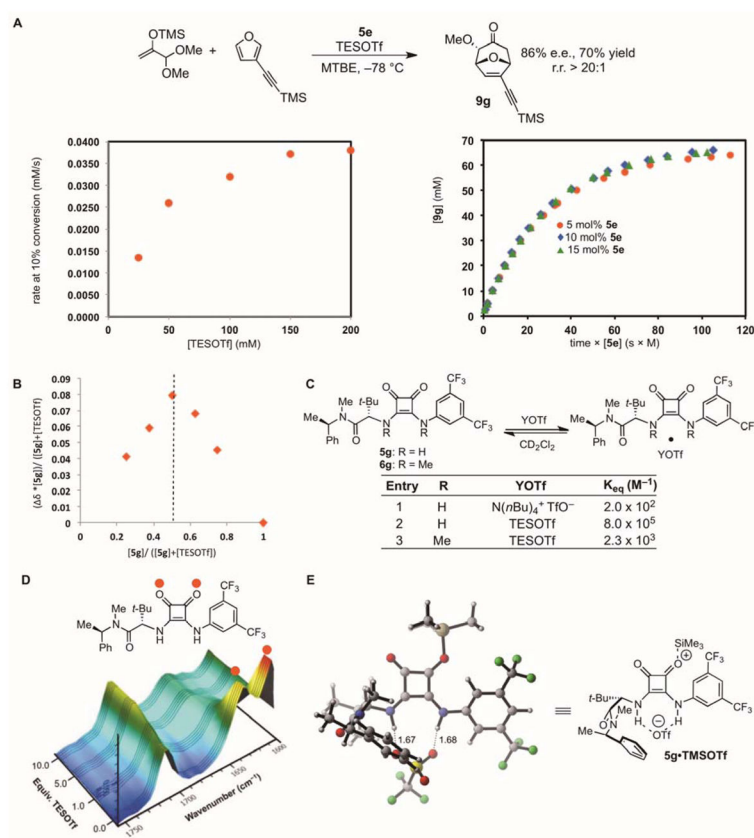


Figure 3. Mechanistic studies

(A) Kinetic analysis of a model (4+3) cycloaddition reaction promoted by **5e**. The reaction rate obeys a first-order dependence on **[5e]** as determined using the Burés method, and displays saturation in **[TESOTf]**. (B) Job plot for the binding of TESOTf to **5g** indicating a 1:1 binding stoichiometry. (C) Equilibrium constants for the binding of **5g** with NBu_4OTf and TESOTf, and of **6g** with TESOTf. These provide evidence for cooperative binding of TESOTf to **5g**. Experiments were conducted at 23 °C in CD_2Cl_2 . (D) IR spectra monitoring addition of TESOTf to catalyst **5g** at -78 °C in MTBE. (E) Lowest-energy ground state structure of **5g** bound to TMSOTf. Calculations were performed at the B3LYP/6-31G(d) level. Structures of alternative, higher-energy complexes are provided in Fig. S22.

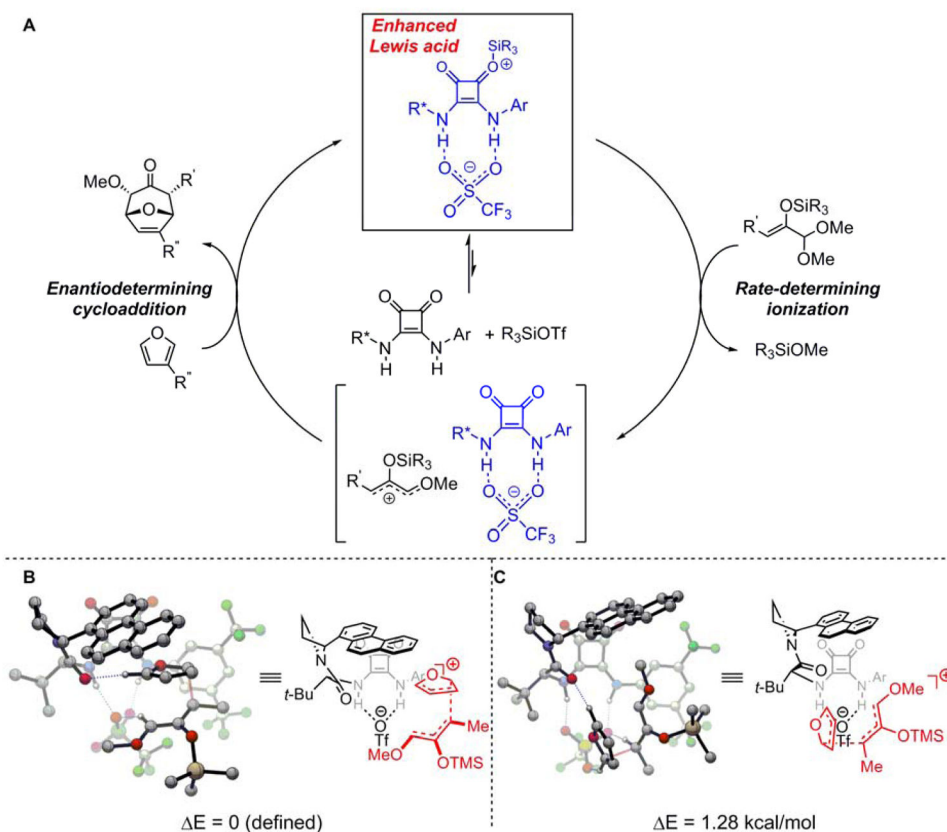


Figure 4. Proposed mechanism

(A) Proposed catalytic cycle for the enantioselective, catalytic (4+3) reactions with $5 \cdot R_3SiOTf$ acting as an enhanced Lewis acid. (B) Lowest-energy transition structure for the first, selectivity-determining C–C bond-forming step in the addition of furan to an oxallyl cation intermediate, leading to the experimentally observed major enantiomer. (C) Corresponding transition structure leading to the minor enantiomer. All distances are in Å. Structures were calculated at the B3LYP/6-31G(d) level of theory, with uncorrected electronic energies at the M062x/6-31+G(d,p) level.